Molecular Therapy
Methods & Clinical Development
Original Article

Transcutaneous Ultrasound-Mediated Nonviral Gene Delivery to the Liver in a Porcine Model

Dominic M. Tran,[1,6] Feng Zhang,[2,6] Kyle P. Morrison,[3] Keith R. Loeb,[4] James Harrang,[1] Masaki Kajimoto,[1] Francisco Chavez,[3] Li Wu,[1] and Carol H. Miao[1,5]

[1]Center for Immunity and Immunotherapies, Seattle Children's Research Institute, Seattle, WA 98101, USA; [2]Department of Radiology, University of Washington, Seattle, WA 98195, USA; [3]Sonic Concepts, Inc., Bothell, WA 98011, USA; [4]Fred Hutchinson Cancer Research Center, Seattle, WA 98109, USA; [5]Department of Pediatrics, University of Washington, Seattle, WA 98195, USA

Ultrasound (US)-mediated gene delivery (UMGD) of nonviral vectors was demonstrated in this study to be an effective method to transfer genes into the livers of large animals via a minimally invasive approach. We developed a transhepatic venous nonviral gene delivery protocol in combination with transcutaneous, therapeutic US (tUS) to facilitate significant gene transfer in pig livers. A balloon catheter was inserted into the pig hepatic veins of the target liver lobes via jugular vein access under fluoroscopic guidance. tUS exposure was continuously applied to the lobe with simultaneous infusion of pGL4 plasmid (encoding a luciferase reporter gene) and microbubbles. tUS was delivered via an unfocused, two-element disc transducer (H105) or a novel focused, single-element transducer (H114). We found applying transcutaneous US using H114 and H105 with longer pulses and reduced acoustic pressures resulted in an over 100-fold increase in luciferase activity relative to untreated lobes. We also showed effective UMGD by achieving focal regions of $>10^5$ relative light units (RLUs)/mg protein with minimal tissue damage, demonstrating the feasibility for clinical translation of this technique to treat patients with genetic diseases.

INTRODUCTION

The liver is a desirable target to treat a number of diseases because it is a main contributor in several metabolic pathways and production of serum proteins. Ultrasound (US)-mediated gene delivery (UMGD) has emerged as an effective gene transfer approach with great clinical relevancy and translational potential to treat various diseases.[1–6] The technique has been applied to deliver genes and therapeutic agents to liver[7–9] and various other tissues that are notoriously difficult to access, such as brain,[10–13] bone,[14,15] myocardium,[16] skeletal muscle,[17,18] and salivary glands.[19] Other gene delivery methods such as DNA-packaged nanoparticle delivery face the challenge of crossing the nuclear envelope for DNA transcription. Effective UMGD relies on sonoporation events caused by exogenous cavitation nuclei such as microbubbles (MBs). MBs oscillate radially under US exposure at particular frequencies and peak negative pressures (PNPs) that can result in transient pores in cell membranes and opening of endothelial tight junctions. Nonviral vectors, such as naked plasmid DNA (pDNA) carrying a gene of interest, diffuse across the temporarily disrupted barrier and enter the nucleus to be transcribed. Our interest lies in developing US technology and minimally invasive techniques to improve nonviral UMGD to liver tissue in order to treat human diseases.

Our recent studies achieved significant gene delivery enhancement in the liver using UMGD via a laparotomic procedure in small- and large-animal models.[8,20–22] Furthermore, we improved gene transfection efficiency using novel US transducer designs and beam patterns, as well as US treatment safety by modifying US protocols using longer pulse durations and lower PNPs.[9] In order to translate our recent findings into a clinically relevant minimally invasive approach, we developed an interventional radiological procedure to facilitate transcutaneous UMGD. However, gene transfer efficiency can be reduced because of the challenge of overcoming acoustic output attenuation across multiple tissue layers (J.H., S. Song, D.M.T., K.R.L., R.Y. Fu, B.M. Smith, et al., unpublished data).[23] Here, we showed the successful optimization of US transducers and protocols in combination with a minimally invasive, transhepatic venous approach to deliver pDNA into target liver lobes to overcome transcutaneous attenuation of US intensity while maintaining effective gene delivery.

RESULTS

Development of a Minimally Invasive Technique for UMGD

Via a trans-jugular-venous approach, a balloon catheter was placed in the hepatic vein of a targeted liver lobe with fluoroscopic imaging guidance. An angiography of the hepatic venous system (Figure S1A) carried out via a terminal procedure in one pig provided reference for the targeted catheter insertion. After catheter placement, the balloon was inflated to occlude blood outflow, followed by injection of X-ray contrast agent into the liver lobe to visualize where the pDNA and MBs would distribute (Figure 1A). Afterward, MBs were perfused distal to the inflated balloon through the catheter,

Received 14 May 2019; accepted 14 July 2019;
https://doi.org/10.1016/j.omtm.2019.07.005.

[6]These authors contributed equally to this work.

Correspondence: Carol H. Miao, Center for Immunity and Immunotherapies, Seattle Children's Research Institute, 1900 Ninth Avenue, Seattle, WA 98101, USA.
E-mail: carol.miao@seattlechildrens.org

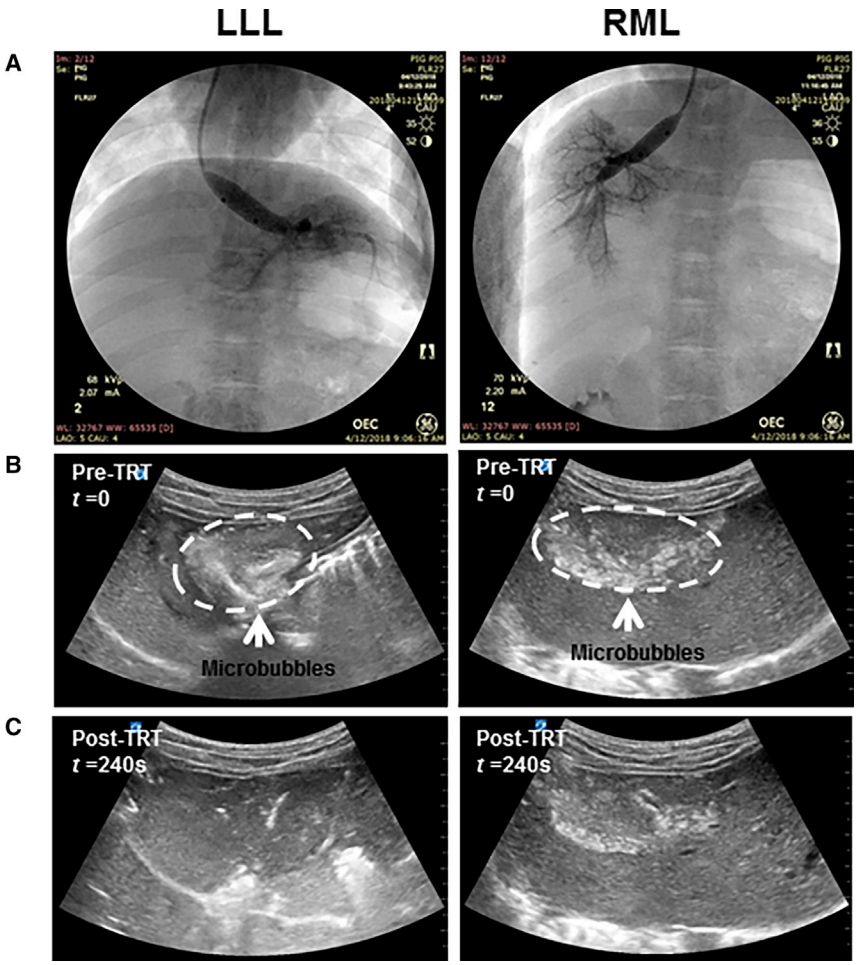

Figure 1. Fluoroscopy-Guided Transhepatic Venous Infusion of Plasmid DNA with MBs in the Left Lateral Lobe (LLL) and Right Medial Lobe (RML)

(A) Angiography of the left and middle hepatic vein confirmed the location of the balloon catheter and where the microbubbles and pDNA infused through the same balloon catheter would distribute. (B and C) Representative ultrasonography of MBs present in the hepatic vasculature before tUS treatment (B) and after treatment (C), showing the distribution of MBs in the liver lobe corresponding to the distribution of X-ray contrast (Visipaque) (B) and the significant decrease of microbubbles in the vasculature post US treatment (C).

and their retention and distribution were examined by diagnostic US imaging (Figure 1B). Transcutaneous diagnostic imaging also helped guide the entry point of the therapeutic US (tUS) beam across the abdominal wall (Figure S2) and direct tUS energy toward the localized, MB-, and pDNA-perfused lobe. tUS was applied to the targeted liver lobe for 4 min followed by diagnostic US imaging to visualize the retention of MBs in the vasculature (Figure 1C). US images demonstrated MBs distributed in the left lateral segment approximately 30–40 mm deep from the entry point of the US beam on the skin, 20–30 mm in the right middle segments, and approximately 40–60 mm deep within the right lobe. The hepatic veins and their segmental branches could be consistently catheterized without major peri-procedural complications (Figures S1B and S1C).

Development of tUS Transducers for Transcutaneous UMGD

Although focused transducers in earlier pig experiments (H185 series) improved gene delivery in laparotomic procedures,[22] they produced low levels of transgene expression in preliminary transcutaneous experiments (data not shown). As a result, a new focused transducer, H114, was designed with an increased linear focal pressure gain of 4.46 and an increased focal depth of 45 mm. The focal length was geometrically increased by equipping a single curved element to produce PNPs $\geq$12 MPa at the focus. An applied center frequency of 1.05 MHz was used to ensure maximal power conversion efficiency of the transducer and US wave propagation to deeper tissue sites.

The performance of H114 was compared with that of transducer H105, which had been used in prior UMGD experiments. H105 is an unfocused, dual-element apodized transducer with a planar surface that is driven at a center frequency of 1.10 MHz. Pressure field profiles of H105 and H114 are shown and compared in Figure 2. Relative pressure outputs across the US beam were measured at various distances using a 1-mm-diameter hydrophone normalized to 1-MPa peak pressure. The pressure field profile of H105 shows non-uniform PNP output transaxially. Due to its unfocused nature, the relative pressure distribution is nearly constant with respect to depth when comparing the two slices at 25 and 45 mm. However, the pressure field profile of H114 indicates transaxial uniformity of PNP output at 25 and 45 mm from the exit plane of the transducer. It should be noted that during transcutaneous US treatment, PNP is expected to decrease because of the presence of multiple skin and tissue layers above the liver. As assessed from our previous simulation model, the attenuated PNPs at acoustic maximum (Amax) during transcutaneous US treatment were estimated to decrease by 50% in intensity and are listed in Table 1. Reported PNPs are approximated derated values. Real-time acoustic output could not be measured during experiments in live pigs, hence electrical input was held constant, as well as pulse duration.

Gene Transfer Enhancement via Transcutaneous UMGD in Porcine Livers

Additional US protocols utilizing lower PNP settings with longer pulse durations were investigated to determine whether efficient UMGD can be achieved using both a focused and an unfocused

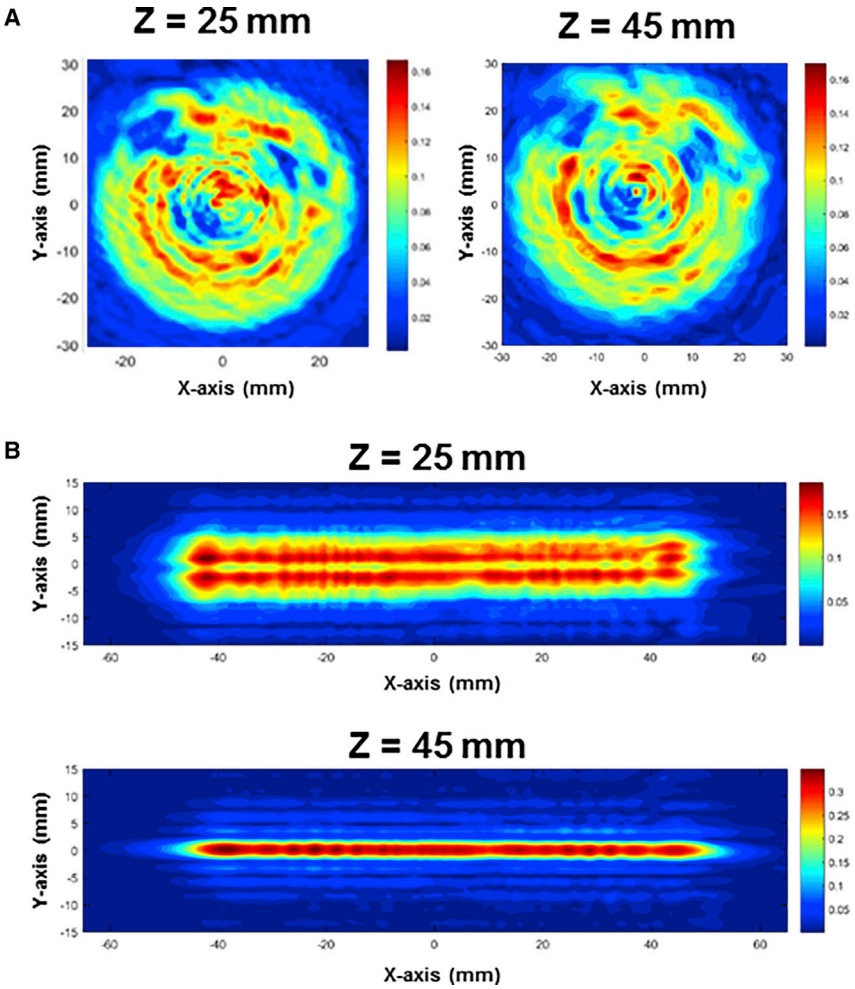

Figure 2. Pressure Profile Maps of H105 and H114 Show Differences in Beam Pattern and Transaxial Uniformity

(A and B) H105 is a planar, disc transducer shown in (A) with pressure profiles at depths of 25 (left) and 45 mm (right). H114 is a geometrically focused transducer shown in (B) with pressure profiles at depths of 25 (top) and 45 mm (bottom). Color gradients reflect relative pressure where warmer colors indicate higher relative pressure and cooler colors indicate lower relative pressure.

transducer while reducing tissue damage (Table 1). The left lateral or right medial or right lateral hepatic lobe of pigs was treated, and the luciferase activity levels in liver tissue were evaluated. The luciferase activity levels in UMGD-treated lobes were compared with untreated lobes without direct tUS exposure. The left medial lobe served as an intra-animal control and was always chosen as the untreated lobe because it was the most difficult to access. The liver lobes were excised 24 h after UMGD, then mapped based on Cartesian coordinates, sampled, and assayed for level of luciferase activity.

There were several points of gene transfer resulting in greater than 10,000 relative light units (RLUs)/mg protein for each US treatment group. Sections with luciferase activity were pooled across pigs for a particular US treatment group and compared (Figure 3). N is the sample size of pigs used, and n is the sample size of tissue sections collected for a particular US protocol among the treated pigs with outliers removed. The untreated liver lobes had luciferase activity values less than 200 RLUs/mg protein (N = 3, n = 26). Using H114, the treatment group at 19 μs, 5.1 MPa had a maximum activity value of 13,291 RLUs/mg protein, a mean value of 3,638 ± 3,324 RLUs/mg protein (N = 2, n = 16), and about a 90-fold increase on average above background; the treatment group at 200 μs, 2.5 MPa had a maximum activity value of 18,046 RLU/mg protein, a mean value of 5,537 ± 4,748 RLU/mg protein (N = 4, n = 55), and about 300-fold increase on average above background; the treatment group at 2 ms, 1.7 MPa had a maximum activity value of 31,509 RLUs/mg protein, a mean activity value of 6,361 + 7,435 RLUs/mg protein (N = 2, n = 47), and a nearly 600-fold increase on average above background. Using H105, the treatment group at 19 μs, 2.2 MPa had a maximum activity value of 8,709 RLU/mg protein, a mean value of 6,260 ± 1,944 RLUs/mg protein (N = 1, n = 8), and about a 150-fold increase on average above background; the treatment group at 200 μs, 1.2 MPa had a maximum activity value of 34,689 RLUs/mg protein, a mean value of 12,020 ± 10,959 RLUs/mg protein (N = 3, n = 39), and about a 330-fold increase on average above background; the treatment group at 2 ms, 0.8 MPa had a maximum activity value of 18,465 RLUs/mg protein, a mean value of 6,168 ± 6,137 RLUs/mg protein (N = 2, n = 34), and also about a 330-fold increase on average above background. All treatment groups achieved significantly greater gene transfer than the untreated group ($p < 0.0001$), and almost all produced at least an over 100-fold increase in gene transfer relative to naive. When comparing among the three treatment groups for either transducer, there was no statistically significant difference in luciferase activity levels (Figure 3). The spread of the data including outliers is shown in Figure S3. Luciferase expression profile maps with plotted sections assayed for luciferase activity are shown in Figure 4. Luciferase expression maps for other US protocols and transducers used are shown in Figure S4. The distribution of luciferase activity on the expression plots was cross-referenced to corresponding fluoroscopy images from the same experiment. The location of the main branch of the accessed hepatic vein provided a reference point to correlate the fluoroscopic image to the luciferase expression plot. The resulting expression maps validate the distribution of contrast agent in targeted liver lobes for all US treatment groups.

Table 1. US Protocols and Transducer Used for Each Treatment Group

Group	Transducer	Frequency (MHz)	Amax (mm)	Focal Gain	PNP[a] (MPa)	Derated PNP[b] (MPa)	Pulse Duration	Duty Cycle (%)	n[c]
1	H105	1.10	35	–	3.1	2.2	19 μs	0.1	8
2	H105	1.10	35	–	1.7	1.2	200 μs	1	39
3	H105	1.10	35	–	1.2	0.8	2 ms	10	34
4	H114	1.05	45	4.46	7.2	5.1	19 μs	0.1	16
5	H114	1.05	45	4.46	3.5	2.5	200 μs	1	55
6	H114	1.05	45	4.46	2.4	1.7	2 ms	10	47

[a]PNPs at acoustic maximum (Amax) from exit plane in the near field (<60 mm) for each transducer were measured by a 1-mm hydrophone in degassed water.
[b]Derated PNP at Amax was estimated assuming attenuation of 50% US intensity through multiple tissue layers.
[c]n denotes the number of tissue sections analyzed.

Histological Assessment of UMGD Using a Highly Focused and Unfocused Transducer

Livers were harvested to examine the potential hepatic injury 24 h after UMGD. Histology samples were taken from areas targeted by US treatment. Although the majority of the liver tissues are normal without any damages in all treated pigs using different protocols, limited liver tissue sections showed damages 1 day after the treatment. There was focal hepatic injury (hemorrhage and necrosis) in several of the samples present in a pericentral distribution around the central vein in the center of the hepatic lobules. The pattern of injury was limited to a few hepatic lobules with varying amounts of pericentral damage that did not involve the portal tracts or bridge between adjacent hepatic lobules. Selected trichrome-stained liver sections from control and US-treated pigs focusing on the area of maximal injury are shown in Figure 5. All of the biopsies including the untreated lobes had mild central venous congestion and hepatic sinusoidal dilation presumably related to the recent therapy (transient venous outflow obstruction during pDNA and MB administration). Using H114, the treatment group at 19 μs, 10 MPa presented no notable tissue damage or injury (Figure 5B). The treatment group at 200 μs, 6 MPa presented with very small areas of pericentral necrosis involving approximately 10% of the hepatic lobules and only 2% of the total tissue from the targeted area (Figure 5C). The treatment group at 2 ms, 4 MPa also showed some pericentral necrosis in two adjacent lobules, representing 7% of the hepatic lobules and 3% of the tissue biopsy (Figure 5D). Using H105, the treatment group at 19 μs, 2 MPa presented with focal injury in four hepatic lobules representing 10% of the total hepatic lobules examined and representing less than 3% of the biopsied tissue (Figure 5E). The treatment group at 200 μs, 1.5 MPa presented with a greater amount of hepatic injury in which 30% of the hepatic lobules were injured, representing approximately 10% of the biopsied tissue (Figure 5F), whereas the treatment group at 2 ms, 1 MPa had focal hemorrhage without notable hepatic injury (Figure 5G). The percent of injured hepatic lobules is a measure of the distribution of hepatic injury (focal or diffuse) and may be related to the US focal length of the movement of the probe during the procedure. The extent of total tissue damage is presumably related to the US conditions.

Blood was also collected 24 h post-surgery to assess transaminase levels. No direct correlation between liver damage and US protocol or transducer could be found as two liver lobes were treated, each with a different US protocol and/or transducer, during each surgery. However, alanine transaminase (ALT) levels were calculated to be 56.9 ± 19.5 U/L on average. The minimum ALT value obtained from UMGD-treated pigs was 22 U/L, and the maximum ALT value was 95 U/L. The median ALT value was 56 U/L. Aspartate transaminase (AST) levels were calculated to be 129 ± 106.8 U/L on average. The minimum AST value was 46 U/L, and the maximum AST value was 389 U/L. The median AST value was 74.5 U/L. Normal porcine ALT and AST levels are between 60 and 90 U/L.

DISCUSSION

Procedural safety is an important factor when developing methods for clinical translation. Earlier studies had developed a minimally invasive technique to access a hepatic, region-specific area for gene delivery in large animals for hydrodynamic gene therapy.[24–26] Thus, a multimodal procedure involving fluoroscopic and US imaging guidance was adopted for transhepatic venous, UMGD in the liver to minimize surgical invasiveness.[27–29] Using interventional radiological techniques under fluoroscopic guidance, the right jugular vein was accessed and the balloon catheter was placed in the left and middle hepatic veins sequentially to infuse pDNA into the liver lobes. The inflated balloon in the hepatic veins occluded blood outflow, ensuring long retention of pDNA in liver sinusoids. This offers a sufficient window of time to apply transcutaneous US to the target lobes and promote gene transfection in the liver. We optimized catheter placement to liver lobes that can be targeted by the US beam efficiently in order to maximize gene delivery to the liver cells. No major peri-procedural complications accessing a liver lobe via the hepatic vein branch occurred during our surgeries.

In our previous studies using laparotomic procedures in pigs, we reported gene transfer could be increased using a pulse duration of 19 μs and PNP settings above 2.7 MPa using the focused H185 US transducer series (J.H., S. Song, D.M.T., K.R.L., R.Y. Fu, B.M. Smith, et al., unpublished data).[22] These focused transducers capable of higher PNPs were assessed in comparison with unfocused transducer H105 and showed improved gene delivery, but did not produce similar results in preliminary transcutaneous experiments.[7] The

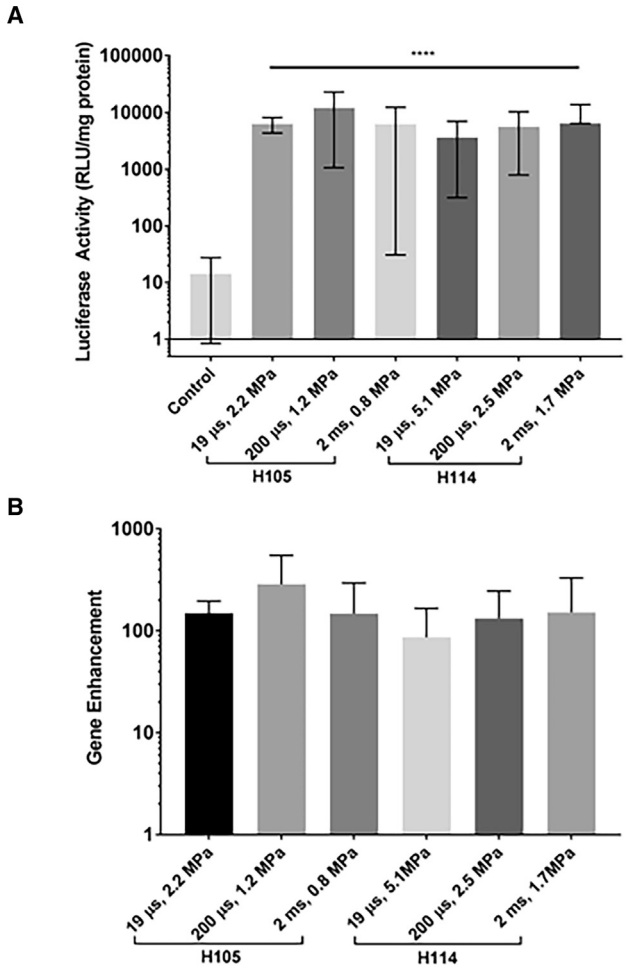

Figure 3. Resulting Luciferase Gene Expression Represented as Activity Levels for H105 and H114 Using Different US Protocols

Data from multiple pigs treated with a particular US protocol were pooled for analysis. (A) All US protocol groups listed in Table 1 are compared with the control group (no MBs + no US treatment). The following lists the exact number of pigs and tissue sections used for analysis: (control) N = 3, n = 26; (H105: 19 µs, 2.2 MPa) N = 1, n = 8; (H105: 200 µs, 1.2 MPa) N = 3, n = 39; (H105: 2 ms, 0.8 MPa) N = 2, n = 34; (H114: 19 µs, 5.1 MPa) N = 2, n = 16; (H114: 200 µs, 2.5 MPa) N = 4, n = 55; (H114: 2 ms, 1.7 MPa) N = 2, n = 47. ****$p < 0.0001$. Data are shown with upper and lower quartiles with median values. (B) Average gene enhancement using either H105 or H114 for all US protocols. Error bars represent SD.

H185 series US transducers used in laparotomy procedures were designed to have a short focal depth (3–20 mm) to scan on the liver surface. Under the transcutaneous US treatment protocol, the liver was located at an increased depth under intervening skin and muscle tissue. In addition, US intensity was attenuated by multiple tissue layers and highly fibrous connective tissue surrounding porcine hepatic lobules, which may dampen the effects of MB cavitation. Therefore, a new, highly focused transducer (H114) capable of producing greater PNPs at a deeper focus was developed for transcutaneous UMGD. Considering that a focused transducer could reduce potential treatment area and volume, the focused transducer, H114, was compared with the unfocused transducer, H105, to determine whether treatment area may be a factor impacting gene transfer.

The luciferase activity assay results suggest that continuous nutation or pivoting of the focused transducer (H114) to scan the target liver lobe is able to facilitate gene transfer to a substantial fraction of a treated lobe, despite that transducer having a narrow focus approximately the width of a grain of rice. Interestingly, although our sample size was limited and direct comparison is not possible, prolonged pulse durations and lower PNP settings appeared to result in equivalent gene transfer as compared with short pulse duration and high PNP settings, similar to our previous studies (J.H., S. Song, D.M.T., K.R.L., R.Y. Fu, B.M. Smith, et al., unpublished data).[9] Both transducers were capable of producing $>10^5$ RLUs/mg protein using longer pulse durations and lower PNPs. These results are nearly similar to Kamimura et al.[30] using hydrodynamic gene delivery where 100- to 1,000-fold increases above untreated lobes were achieved. The length of energy deposition over time with prolonged pulse durations may be a contributing factor. Although not examined here, other studies demonstrated that as pulse duration is increased and PNP decreased, there is a higher likelihood that MBs will experience stable cavitation, enhancing mechanical influences on the cells.[31–33] The stress-induced oscillatory effect can be advanced by using targeted, pDNA-bound MBs to improve gene delivery, and it is planned for future studies. These results suggest the importance of both treatment volume and US protocol design for UMGD efficiency. A limitation to the work presented is the inability to assess the average gene expression as a function of depth using both transducers. Here also only intra-animal controls were used by comparing untreated lobes with tUS-treated lobes. There is a possibility that the untreated lobes were exposed to reflected US. However, the effects on actual gene transfer are considered to be negligible as evidenced by the low luciferase activity detected in these untreated lobes. This is due to restrictions in material cost and labor given the large size of each pig's liver. Potential improvements in transducer design can be made by combining features of H114 and H105 to produce sufficiently high PNPs while maintaining a larger treatment area for greater coverage and delivery efficacy. One design could involve segmenting H114's single cylindrical element into a multi-channel array in order to allow variable defocusing of the US beam while maintaining high PNP outputs.

To manage the safety profile of US energy deposition, both H105 and H114 were continuously scanned across the target in an attempt to minimize focal damage from prolonged exposure as explained by Watkin et al.[34] Although the majority of the liver sections are normal via histological analysis, all treatment groups revealed some liver tissue damage in limited liver sections. More studies are required to affirm resulting damages from use of certain US protocols and transducers and to allow comparison between groups. Furthermore, liver transaminase (ALT and AST) levels in US-treated pigs at day 1 were either normal or slightly elevated, indicating minor liver damages. These physical damages were repaired quickly after a few days as shown in our previous long-term rat studies,[8] in contrast with

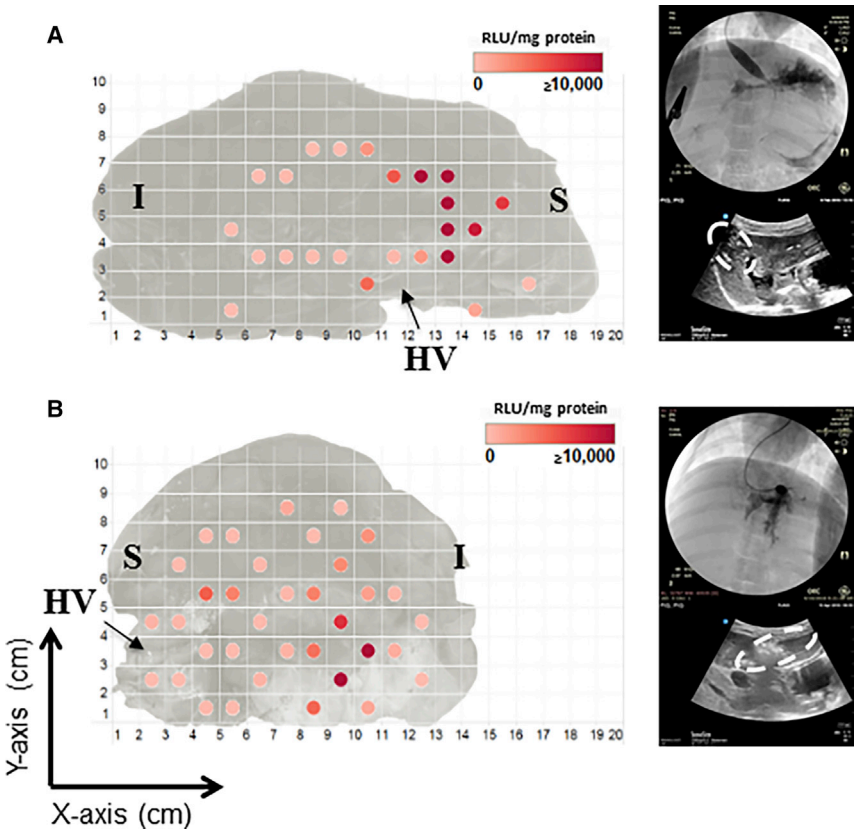

Figure 4. Luciferase Expression Distribution Plots Validating Catheter Placement within Target Hepatic Lobe

(A and B) Resulting luciferase activity level for assayed tissue sections overlaid onto a mapped plot of the liver lobe is shown. Black arrows indicate location of HV used for cross-reference to correlate fluoroscopy images to luciferase expression maps. Increasing luciferase expression corresponds to a shift in color shade from light to dark with the range of expression levels indicated in the color bars (0 to ≥ 10,000 RLU/mg protein). Spatial gene distribution maps are shown according to transducer and US protocol used: (A) H114 (200 μs, 2.5 MPa) and (B) H105 (200 μs, 1.2 MPa). Corresponding fluoroscopy images are shown to the right of the spatial distribution maps. This spatial distribution qualitative analysis was performed for every liver lobe assayed, for a total of 31 liver lobes. S represents superior and I represents inferior relative to the head and tail of the pig. HV, hepatic vein (placed where the main branch of the hepatic vein is located).

potential induction of long-term side effects observed from viral vector-mediated gene transfer.

In conclusion, our study showed the feasibility of performing minimally invasive, nonviral UMGD to the liver in a transcutaneous, clinically relevant setting. Most importantly, our study demonstrated that prolonged pulse duration allowed us to use lower acoustic pressures for efficient gene delivery while applying transcutaneous US across several tissue layers. With these successes, we overcame significant limitations in scaling-up including acoustic attenuation through multiple tissue layers, increased treatment area and volume, and potential tissue damage via UMGD to achieve efficient gene transfer in large animals. Ongoing work continues to explore delivery of therapeutic pDNA via transcutaneous UMGD in large-animal models, which may pave the way toward translating the technology of minimally invasive, nonviral UMGD to the clinic.

MATERIALS AND METHODS

Animal Use Protocol

All procedures were performed according to the guidelines for animal care of the NIH and Seattle Children's Research Institute (SCRI), with protocol approval of Institutional Animal Care and Use Committees of both SCRI and the University of Washington. Specific-pathogen-free (SPF)-derived Yorkshire hybrid swine (13–24 kg) were obtained from S&S Farms (Ramona, CA, USA). The swine were acclimated for at least 4 days prior to treatment.

Plasmid and MB Preparation

The luciferase reporter plasmid pGL4.13 [luc2/SV40] (Promega, Madison, WI, USA) was produced by GenScript (Piscataway, NJ, USA) according to standard industry techniques. Preparation of RN18 MBs was described previously by Sun et al.[35] In brief, the MB shells were composed of lipids at a 82:10:8 molar ratio of 1, 2-distearoyl-*sn*-glycero-3-phosphocholine (DSPC), 1,2-distearoyl-*sn*-glycero-3-phosphate (DSPA), and *N*-(carbonylmethoxypolyethyleneglycol 5000-DSPE) (Avanti Polar Lipids, Alabaster, AL, USA). The lipids were reconstituted, and gas exchange was performed with the headspace filled with octafluoropropane gas (American Gasp Group, Toledo, OH, USA). MB size and concentration were measured using the qNano with a NP2000 membrane and calibrated with CPC1000 particles (Izon Science, Christchurch, New Zealand), and analyzed using the accompanying Izon V3.3 software. Before use, MBs were activated by vigorous agitation for 45 s using a Vialmix (Lantheus Medical Imaging, North Billerica, MA, USA), yielding an average concentration of 2–5 × 10^9 MBs/mL.

US Transducers and Systems

The US system was previously described by Noble et al.[7] In this system, a laptop was used to control the signal-generating amplifiers (Model: RFG-1500BB [JJ&A Instruments, Duvall, WA, USA] and Model: RPR-4000-HP [Ritec, Warwick, RI, USA]) capable of producing up to 1.5 and 15 kilowatts (KW) of electrical power, respectively, via a custom serial interface (Sonic Concepts, Bothell, WA, USA). The combined pulse generator and radio-frequency amplifier was connected to an impedance matching network to minimize reflections

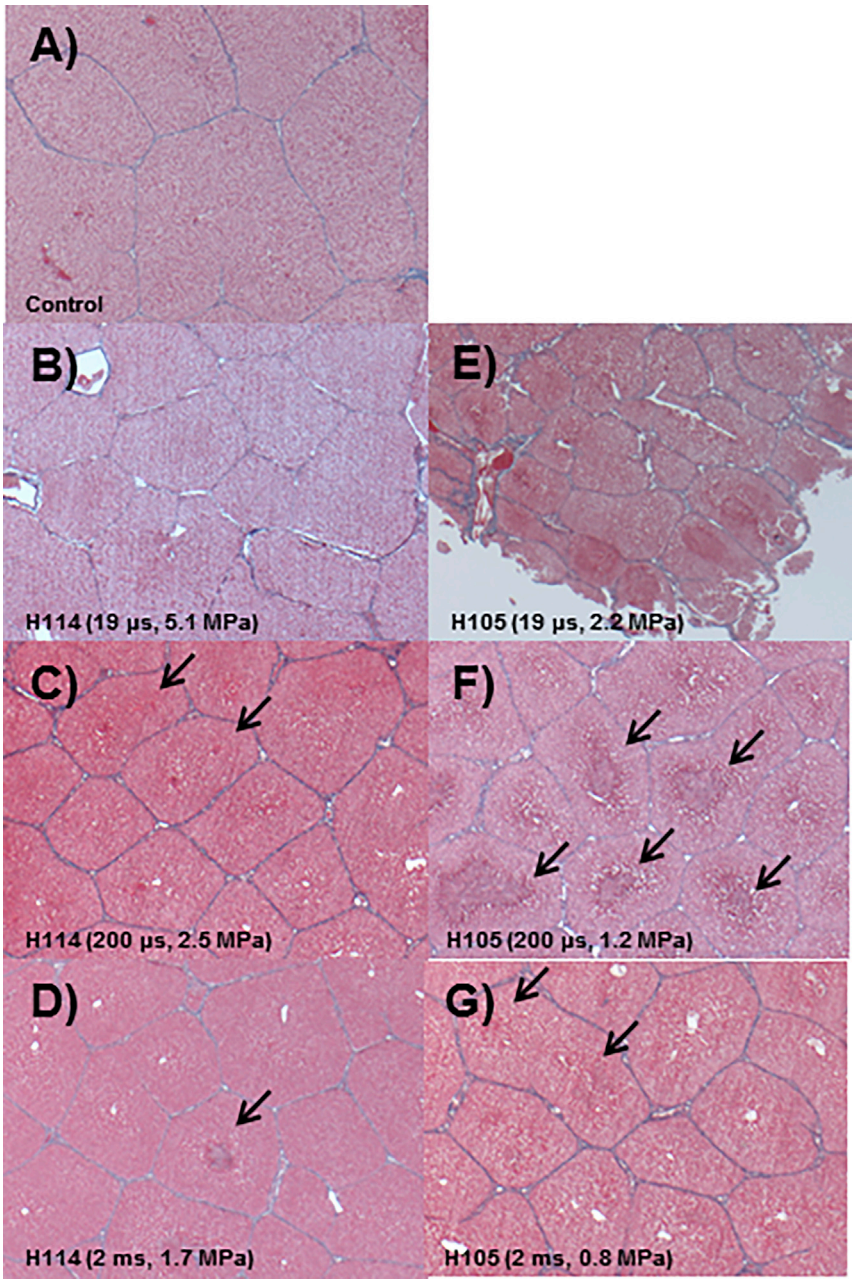

Figure 5. Selected Trichrome-Stained Liver Sections with the Maximal Damages in Pigs Treated with Different US Protocols

No damage was observed in the majority of the liver section in all treated pigs. Trichrome-stained slides of limited liver sections focusing on the area of maximal hepatic damage for all treatment groups according to transducer and US protocol used, including control, are shown: (A) untreated control lobe; (B) H114 (19 µs, 5.1 MPa); (C) H114 (200 µs, 2.5 MPa); (D) H114 (2 ms, 1.7 MPa); (E) H105 (19 µs, 2.2 MPa); (F) H114 (200 µs, 1.2 MPa); and (G) H114 (2 ms, 0.8 MPa). Black arrows point to areas of pericentral hemorrhage and necrosis. The histological analysis was shown at ×2.5 original magnification.

and maximize power transfer. The matching network is subsequently connected to either a dual-element, 57-mm diameter, unfocused disc transducer (Model H105; center frequency = 1.10 MHz; Sonic Concepts) or a single-element, focused transducer (Model H114; center frequency = 1.05 MHz; Sonic Concepts). The focus of H114 lies at 45 mm from the exit plane with a focal pressure gain of 4.46. Spatial average PNPs used with H105 ranged from 1.2 to 3.1 MPa. Spatial average PNPs used with H114 ranged from 2.4 to 7.2 MPa after including the focal gain. Derated PNP at Amax (Table 1) was estimated assuming attenuation of 50% US intensity through multiple tissue layers. US was delivered using a 50-Hz pulse repetition frequency for 4 min of total US exposure.

Porcine Surgery

All procedures were performed according to the guidelines for animal care of both the NIH, SCRI, and the University of Washington, with protocol approval of the Institutional Animal Care and Use Committee. The surgeons and veterinary staff were blinded to US protocol allocation for each pig. However, the tUS operators were not blinded because this was not possible. After administration of preanesthetic (acepromazine: 1.1 mg/kg) and induction of general anesthesia (ketamine: 33 mg/kg, glycopyrrolate: 0.005 mg/kg), each pig (15–18 kg) was placed in supine position and maintained in a stable anesthetic plane with isoflurane. The abdomen was shaved before positioning to allow better coupling between the transducer and transmission gel. The pig was draped in a sterile fashion. A micropuncture introducer set (Cook Medical, Bloomington, IN, USA) was used to access the right jugular vein under US imaging guidance (X-Porte; FUJIFILM Sonosite, Bothell, WA, USA). An 8 Fr sheath (Boston Scientific) was then placed into the vein and sutured in place. A NIH angiographic catheter (Cook Medical) was placed through the sheath to cross the right atrium of the heart and access the inferior vena cava. Fluoroscopy (OEC 9900 Elite C-arm X; GE Healthcare, Little Chalfont, UK) was used to verify the placement of the angiographic catheter. The angiographic catheter was positioned to the desired target liver lobe via a hepatic vein branch, and a Back-Up Meier C-Tip guidewire (Boston Scientific) was inserted for introducing a balloon catheter (20.0-mm length and 12.0-mm diameter). X-ray contrast agent (Visipaque; GE Healthcare) was injected to verify the position of the catheter. The balloon was inflated to occlude the blood outflow from the hepatic

venous branch. A pGL4/MB solution (2 mL/kg solution containing 0.67 mg/kg pGL4, 0.1 mL/kg MBs, 0.2 mL/kg 50% glucose, and PBS to total weight-based volume) was injected to the occluded hepatic region. Transcutaneous tUS was delivered simultaneously to the injected lobe for 4 min. The MB distribution in the target liver lobe was visualized by US imaging using a C60xp transducer (bandwidth = 2–5 MHz) connected to the SonoSite X-Porte before and after US treatment. This allowed us to verify the location of pGL4/MB solution and the required direction of US energy via the therapeutic transducer before treatment, as well as to determine whether MB destruction occurred after treatment. After the US treatment, catheters were removed and the incision was closed using sutures. The pigs were allowed to recover. Post-operative systemic analgesics were administered (ketoprofen: 2 mg/kg, buprenorphine: 0.02 mg/kg). Physiological parameters including heart rate, oxygen saturation (SpO2), body temperature, and systolic and diastolic blood pressure for the pig were monitored throughout the surgery by a licensed veterinary technician. After 24 h, the pigs were sacrificed, and the treated and control lobes were harvested for sectioning and processing for luciferase expression. Blood and tissue samples were collected for liver enzyme and histological analysis.

Hepatic Venography

Under anesthesia (acepromazine: 1.1 mg/kg, glycopyrrolate: 0.005 mg/kg, 3% isoflurane), a balloon catheter (Boston Scientific, Marlborough, MA, USA) is threaded into the jugular vein and the inferior or caudal vena cava to a level cranial to the liver of the pig. A laparotomy was performed to expose the main portal vein. The portal vein was then cannulated to allow a guidewire to be placed, over which an 8 Fr sheath was inserted into the vessel. The main portal vein was then ligated to secure the sheath. A total of 60,000 units of heparin saline was perfused via the inferior vena cava (IVC) caudal to the liver to flush the blood from the hepatic venous system. The balloon catheter was then inflated to occlude the IVC cranial to the liver. The IVC caudal to the liver was ligated and the body wall closed. X-ray contrast agent (Visipaque; GE Healthcare) in saline was infused into the IVC and hepatic venous system via the balloon catheter. A venogram of the hepatic venous system was then obtained using an OEC 9900 Elite C-arm X-ray machine (GE Healthcare), and the pig was euthanized thereafter.

Luciferase Gene Expression Analysis

All liver lobes were resected following sacrifice of the pig 24 h after the procedure when the pGL4 luciferase expression reaches the peak level as experimentally determined before. The control lobe is defined as lobes without having directly been injected with the pGL4/MB solution and not exposed to tUS. Treated and control lobes were spatially mapped and sectioned into smaller pieces, and some samples were assayed for luciferase expression as previously described (J.H., S. Song, D.M.T., K.R.L., R.Y. Fu, B.M. Smith, et al., unpublished data).[22] In brief, supernatant was collected from homogenate that underwent several freeze-thaw cycles, and its luciferase activity was analyzed using a commercially available kit (Luciferase Assay System, Promega, Madison, WI, USA) and measured by a luminometer (Victor 3; Perkin Elmer, Wellesley, MA, USA). Luciferase expression was normalized to total protein content, measured by BCA assay kit (Bio-Rad, Hercules, CA, USA), and reported as RLUs per milligram protein.

Blood Analysis

To detect liver damage after treatment, blood samples were collected before euthanasia and sent to a commercial veterinary diagnostic laboratory (Phoenix Central Laboratory, Mukilteo, WA, USA) for a complete blood count and a chemistry panel including ALT and AST values.

Histological Analysis

Treated and control liver biopsies were fixed in 10% neutral-buffered formalin, then processed and embedded in paraffin. Routine H&E and trichrome-stained slides were made to examine any liver damage. H&E and trichrome slides were examined by a qualified pathologist (K.R.L.) who was blinded to the treatment administered.

Statistical Analysis

All data are presented as means with SD or medians with upper and lower quartiles, as well as maximums and minimums. An adequate number of tissue sections is believed to have been collected to cover analysis of roughly 50% or more of the liver lobe. Statistical methods were not used to predetermine sample size. Data gathered from multiple liver lobes treated with the same US protocol and transducer from different pigs were pooled. To differentiate between treated and non-treated tissue sections, a maximum-to-minimum luciferase activity ratio was calculated from untreated liver lobes to provide a background threshold ratio. Tissue sections were considered treated if the luciferase activity value surpassed the threshold ratio. Outliers were identified and removed from the pooled data using the regressin and outlier removal (ROUT) method from a statistical package (GraphPad Prism 7; Prism, Reston, VA, USA) with Q = 1%. A Kruskal-Wallis single-factor ANOVA was performed using GraphPad and corrected for multiple comparisons using Dunn's test. A Tukey test was also performed post hoc for multiple pairwise comparisons. p values of less than 0.05 were considered to be statistically significant.

SUPPLEMENTAL INFORMATION

Supplemental Information can be found online at https://doi.org/10.1016/j.omtm.2019.07.005.

AUTHOR CONTRIBUTIONS

D.M.T. contributed to experimental design, data acquisition, analysis, interpretation, and manuscript preparation. F.Z. contributed to interventional procedural design, development and implementation, interpretation of data, and manuscript preparation. K.P.M. contributed to experimental design, US equipment design, and interpretation of data. K.R.L. contributed to interpretation and collection of histological data, and draft editing. J.H. contributed to experimental design and data acquisition. M.K. contributed to surgical implementation. F.C. contributed to US equipment design and analysis, production of pressure profile maps, and interpretation of data. L.W. contributed

to experimental design and data acquisition and analysis. C.H.M. contributed to conception and design of the work, surgical implementation, interpretation of data, and manuscript preparation.

CONFLICTS OF INTEREST

The authors declare no competing interests.

ACKNOWLEDGMENTS

We would like to thank Dr. Xiaoming Yang for providing the US imaging equipment. We would also like to thank Dr. Maia Chan, Devin Margolies, Erika Wulfert, Dr. Nicholas Reyes, and Emily Spaulding for their expertise and care in managing the well-being of all animal subjects involved. This work is supported by NIH-National Heart, Lung, and Blood Institute grant numbers NHLBI R01 HL128139 and R33 HL089038.

REFERENCES

1. Miao, C.H., and Brayman, A.A. (2011). Ultrasound-mediated gene delivery. In Non-viral Gene Therapy, X. Yuan, ed. (Intech), pp. 213–242.
2. Price, R.J., Fisher, D.G., Suk, J.S., Hanes, J., Ko, H.S., and Kordower, J.H. (2019). Parkinson's disease gene therapy: will focused ultrasound and nanovectors be the next frontier? Mov. Disord. Published online March 25, 2019. https://doi.org/10.1002/mds.27675.
3. Miao, C.H., Brayman, A.A., Loeb, K.R., Ye, P., Zhou, L., Mourad, P., and Crum, L.A. (2005). Ultrasound enhances gene delivery of human factor IX plasmid. Hum. Gene Ther. *16*, 893–905.
4. Anderson, C.D., Moisyadi, S., Avelar, A., Walton, C.B., and Shohet, R.V. (2016). Ultrasound-targeted hepatic delivery of factor IX in hemophiliac mice. Gene Ther. *23*, 510–519.
5. Manta, S., Renault, G., Delalande, A., Couture, O., Lagoutte, I., Seguin, J., Lager, F., Houzé, P., Midoux, P., Bessodes, M., et al. (2017). Cationic microbubbles and antibiotic-free miniplasmid for sustained ultrasound-mediated transgene expression in liver. J. Control. Release *262*, 170–181.
6. Huang, S., Ren, Y., Wang, X., Lazar, L., Ma, S., Weng, G., and Zhao, J. (2019). Application of Ultrasound-Targeted Microbubble Destruction-Mediated Exogenous Gene Transfer in Treating Various Renal Diseases. Hum. Gene Ther. *30*, 127–138.
7. Noble, M.L., Kuhr, C.S., Graves, S.S., Loeb, K.R., Sun, S.S., Keilman, G.W., Morrison, K.P., Paun, M., Storb, R.F., and Miao, C.H. (2013). Ultrasound-targeted microbubble destruction-mediated gene delivery into canine livers. Mol. Ther. *21*, 1687–1694.
8. Song, S., Noble, M., Sun, S., Chen, L., Brayman, A.A., and Miao, C.H. (2012). Efficient microbubble- and ultrasound-mediated plasmid DNA delivery into a specific rat liver lobe via a targeted injection and acoustic exposure using a novel ultrasound system. Mol. Pharm. *9*, 2187–2196.
9. Tran, D.M., Harrang, J., Song, S., Chen, J., Smith, B.M., and Miao, C.H. (2018). Prolonging pulse duration in ultrasound-mediated gene delivery lowers acoustic pressure threshold for efficient gene transfer to cells and small animals. J. Control. Release *279*, 345–354.
10. Mead, B.P., Kim, N., Miller, G.W., Hodges, D., Mastorakos, P., Klibanov, A.L., Mandell, J.W., Hirsh, J., Suk, J.S., Hanes, J., and Price, R.J. (2017). Novel Focused Ultrasound Gene Therapy Approach Noninvasively Restores Dopaminergic Neuron Function in a Rat Parkinson's Disease Model. Nano Lett. *17*, 3533–3542.
11. Fan, C.H., Lin, C.Y., Liu, H.L., and Yeh, C.K. (2017). Ultrasound targeted CNS gene delivery for Parkinson's disease treatment. J. Control. Release *261*, 246–262.
12. Tan, J.K., Pham, B., Zong, Y., Perez, C., Maris, D.O., Hemphill, A., Miao, C.H., Matula, T.J., Mourad, P.D., Wei, H., et al. (2016). Microbubbles and ultrasound increase intraventricular polyplex gene transfer to the brain. J. Control. Release *231*, 86–93.
13. Timbie, K.F., Mead, B.P., and Price, R.J. (2015). Drug and gene delivery across the blood-brain barrier with focused ultrasound. J. Control. Release *219*, 61–75.
14. Bez, M., Sheyn, D., Tawackoli, W., Avalos, P., Shapiro, G., Giaconi, J.C., Da, X., David, S.B., Gavrity, J., Awad, H.A., et al. (2017). In situ bone tissue engineering via ultrasound-mediated gene delivery to endogenous progenitor cells in mini-pigs. Sci. Transl. Med. *9*, eaal3128.
15. Bez, M., Kremen, T.J., Tawackoli, W., Avalos, P., Sheyn, D., Shapiro, G., Giaconi, J.C., Ben David, S., Snedeker, J.G., Gazit, Z., et al. (2018). Ultrasound-Mediated Gene Delivery Enhances Tendon Allograft Integration in Mini-Pig Ligament Reconstruction. Mol. Ther. *26*, 1746–1755.
16. Chen, S., Chen, J., Meng, X.L., Shen, J.S., Huang, J., Huang, P., Pu, Z., McNeill, N.H., and Grayburn, P.A. (2016). ANGPTL8 reverses established adriamycin cardiomyopathy by stimulating adult cardiac progenitor cells. Oncotarget *7*, 80391–80403.
17. Bastarrachea, R.A., Chen, J., Kent, J.W., Jr., Nava-Gonzalez, E.J., Rodriguez-Ayala, E., Daadi, M.M., Jorge, B., Laviada-Molina, H., Comuzzie, A.G., Chen, S., and Grayburn, P.A. (2017). Engineering brown fat into skeletal muscle using ultrasound-targeted microbubble destruction gene delivery in obese Zucker rats: Proof of concept design. IUBMB Life *69*, 745–755.
18. Chen, S., Bastarrachea, R.A., Shen, J.S., Laviada-Nagel, A., Rodriguez-Ayala, E., Nava-Gonzalez, E.J., Huang, P., DeFronzo, R.A., Kent, J.W., Jr., and Grayburn, P.A. (2018). Ectopic BAT mUCP-1 overexpression in SKM by delivering a BMP7/PRDM16/PGC-1a gene cocktail or single PRMD16 using non-viral UTMD gene therapy. Gene Ther. *25*, 497–509.
19. Wang, Z., Zourelias, L., Wu, C., Edwards, P.C., Trombetta, M., and Passineau, M.J. (2015). Ultrasound-assisted nonviral gene transfer of AQP1 to the irradiated minipig parotid gland restores fluid secretion. Gene Ther. *22*, 739–749.
20. Shen, Z.P., Brayman, A.A., Chen, L., and Miao, C.H. (2008). Ultrasound with microbubbles enhances gene expression of plasmid DNA in the liver via intraportal delivery. Gene Ther. *15*, 1147–1155.
21. Song, S., Shen, Z., Chen, L., Brayman, A.A., and Miao, C.H. (2011). Explorations of high-intensity therapeutic ultrasound and microbubble-mediated gene delivery in mouse liver. Gene Ther. *18*, 1006–1014.
22. Noble-Vranish, M.L., Song, S., Morrison, K.P., Tran, D.M., Sun, R.R., Loeb, K.R., Keilman, G.W., and Miao, C.H. (2018). Ultrasound-Mediated Gene Therapy in Swine Livers Using Single-Element, Multi-lensed, High-Intensity Ultrasound Transducers. Mol. Ther. Methods Clin. Dev. *10*, 179–188.
23. Zderic, V., Keshavarzi, A., Andrew, M.A., Vaezy, S., and Martin, R.W. (2004). Attenuation of porcine tissues in vivo after high-intensity ultrasound treatment. Ultrasound Med. Biol. *30*, 61–66.
24. Khorsandi, S.E., Bachellier, P., Weber, J.C., Greget, M., Jaeck, D., Zacharoulis, D., Rountas, C., Helmy, S., Helmy, A., Al-Waracky, M., et al. (2008). Minimally invasive and selective hydrodynamic gene therapy of liver segments in the pig and human. Cancer Gene Ther. *15*, 225–230.
25. Kamimura, K., Kanefuji, T., Yokoo, T., Abe, H., Suda, T., Kobayashi, Y., Zhang, G., Aoyagi, Y., and Liu, D. (2014). Safety assessment of liver-targeted hydrodynamic gene delivery in dogs. PLoS ONE *9*, e107203.
26. Fabre, J.W., Whitehorne, M., Grehan, A., Sawyer, G.J., Zhang, X., Davenport, M., and Rela, M. (2011). Critical physiological and surgical considerations for hydrodynamic pressurization of individual segments of the pig liver. Hum. Gene Ther. *22*, 879–887.
27. Bashir, S., Mukund, A., Syed, R.F., Nayak, S.L., Rastogi, A., and Sarin, S.K. (2018). Combined Fluoroscopy and Ultrasound-Guided Transjugular Kidney Biopsy in Cirrhotic Patients. J. Vasc. Interv. Radiol. *29*, 696–703.
28. Gebauer, B., El-Sheik, M., Vogt, M., and Wagner, H.J. (2009). Combined ultrasound and fluoroscopy guided port catheter implantation—high success and low complication rate. Eur. J. Radiol. *69*, 517–522.
29. Lee, W., Kim, G.C., Kim, J.Y., Baik, S.K., Lee, H.J., Kim, H.J., and Ryeom, H.K. (2008). Ultrasound and fluoroscopy guided percutaneous transhepatic biliary drainage in patients with nondilated bile ducts. Abdom. Imaging *33*, 555–559.
30. Kamimura, K., Suda, T., Xu, W., Zhang, G., and Liu, D. (2009). Image-guided, lobe-specific hydrodynamic gene delivery to swine liver. Mol. Ther. *17*, 491–499.
31. Fan, Z., Chen, D., and Deng, C.X. (2013). Improving ultrasound gene transfection efficiency by controlling ultrasound excitation of microbubbles. J. Control. Release *170*, 401–413.

32. Mancia, L., Vlaisavljevich, E., Xu, Z., and Johnsen, E. (2017). Predicting Tissue Susceptibility to Mechanical Cavitation Damage in Therapeutic Ultrasound. Ultrasound Med. Biol. *43*, 1421–1440.

33. Helfield, B., Chen, X., Watkins, S.C., and Villanueva, F.S. (2016). Biophysical insight into mechanisms of sonoporation. Proc. Natl. Acad. Sci. USA *113*, 9983–9988.

34. Watkin, N.A., ter Haar, G.R., and Rivens, I. (1996). The intensity dependence of the site of maximal energy deposition in focused ultrasound surgery. Ultrasound Med. Biol. *22*, 483–491.

35. Sun, R.R., Noble, M.L., Sun, S.S., Song, S., and Miao, C.H. (2014). Development of therapeutic microbubbles for enhancing ultrasound-mediated gene delivery. J. Control. Release *182*, 111–120.